



# Study on electrochemical discharge machining of small holes array on glass with ultrasonic vibrating tube electrode

Chenghu Jia<sup>1</sup> · Yong Liu<sup>1,2</sup> · Tianbo Wang<sup>1</sup> · Chengzhi Wang<sup>1</sup> · Kan Wang<sup>1</sup>

Received: 9 April 2023 / Accepted: 6 September 2023 / Published online: 18 September 2023  
© The Author(s), under exclusive licence to Springer-Verlag London Ltd., part of Springer Nature 2023

## Abstract

Electrochemical discharge machining (ECDM), as a new type of non-traditional machining method, is widely used in the machining of insulating hard and brittle materials such as glass and ceramics. However, there are some problems such as difficulty in circulating electrolyte, resulting in poor quality machining of deep and small holes. In this paper, electrochemical discharge machining with ultrasonic vibration and tube electrode is used to improve the flow field in the machining gap and enhance the machining quality by using the injected electrolyte inside the tube electrode and ultrasonic vibration. First, the temperature distribution state of electrochemical discharge is simulated, and the influence of the coupling effect of the electrolyte injection and ultrasonic vibration on the machining gap is analyzed. And then, the influence weights of each factor were analyzed by orthogonal experiments and further analyzed to obtain the optimized combination of machining parameters, which reduced the entrance size of small holes by 19.3%, increased the machining depth by 18.5% and increased the depth-to-diameter ratio by 46.2% compared with the traditional ECDM. The effect of ultrasonic vibration was studied on the basis of the optimized machining parameters. The results show that the optimized effect of ultrasonic vibration with an amplitude of 7  $\mu\text{m}$  is most obvious under the conditions of low pressure and low injection rate. Finally, with the optimized machining parameters, a 5×5 array of small holes and three deep and small holes were machined, demonstrating that electrochemical discharge machining with ultrasonic vibrating tube electrode can be an efficient and high-quality method for machining small holes.

**Keywords** ECDM · Tube electrode · Electrolyte injection · Ultrasonic vibration · Small holes

## 1 Introduction

With high hardness, good light transmission, corrosion resistance, and very low coefficient of thermal expansion, glass materials have a very wide range of applications in the microelectromechanical systems and biomedical industries [1]. However, for materials such as ceramics and glass, the hard and brittle properties can make them susceptible to brittle fracture of the material during conventional machining thereby producing severe surface and subsurface damage and affecting machining accuracy. ECDM, as a non-contact

machining method that uses heat generated by spark discharge to remove workpiece material, is a more ideal way to machine non-conductive hard and brittle materials such as ceramics [2].

Sharma et al. focused on the effect of voltage and feed rate on the depth, overcutting, taper and tool wear of micro-small holes while machining alumina ceramics. Small holes with depth of 228  $\mu\text{m}$  and hole diameter of 270  $\mu\text{m}$  were obtained using optimized set of machining parameters [3]. Singh et al. attempted to machine small holes on silicon wafers and analyzed the effect of voltage and feed rate on the size and taper of small holes. It was found that the hole size and taper increased with increasing voltage and decreased with increasing feed rate [4]. Kolhekar et al. investigated the effect of the state of the gas film on the effect of electrochemical discharge machining. The results showed that the smaller the peak and fluctuation of current, the thinner and more stable the gas film is and the higher the accuracy of the machined hole [5].

✉ Yong Liu  
rzliuyong@163.com

<sup>1</sup> School of Mechanical, Electrical & Information Engineering, Shandong University, Weihai City 264209, People's Republic of China

<sup>2</sup> Weihai Institute of Industrial Technology, Shandong University, Weihai City 264209, People's Republic of China

Sabahi et al. found that the higher the viscosity of the electrolyte, the better the machining accuracy and the smoother the machined surface. In addition, the use of KOH solution reduces the electrode loss compared to NaOH solution, but also deteriorates the surface roughness due to the higher discharge energy [6]. Elhami et al. found that the nanoelectrolyte had enhanced electrical conductivity and thermal conductivity, but the accuracy of the resulting holes was significantly worse because the discharge was too intense [7].

The stability of the tool electrode during machining is very important for ECDM, the high temperature and corrosion resistance determines the consistency before and after machining; therefore, a suitable tool electrode is the key to ensure the machining accuracy. Bian et al. found that when machining with helical electrodes, the temperature field intensity at the sidewall tool edge is higher, and spark discharge is easily formed, and electrode losses are mostly generated from the sidewall tool edge [8]. Sharma et al. experimented with multi-headed tool electrodes for array of holes in silicon-based materials to reduce the number and time of tool electrode machining. It was found experimentally that due to the close distance between the poles of the multi-headed electrodes, the electrodes interfere with each other when generating the gas film and there are differences in electrode losses. The electrode loss at the outermost end is the most serious, and the size of the machined array holes is not consistent due to different discharge states [9].

When machining small holes with large depths, gas bubbles are continuously generated on the sidewalls of the electrode by electrolysis, which makes it difficult to circulate the electrolyte in the machining gap and affects the machining results. Mehrabi et al. used a tube electrode to realize the supply of stable electrolyte into the machining gap during machining, which can provide the gap pressure to bind the gas film and discharge the machining products while making up the electrolyte in time, thus further improving the machining depth. The results show that the electrolyte injection can improve the quality of the gas film and replenish the vaporized electrolyte in the machining gap, thus alleviating the machining discontinuity. And it is proved that the higher the injection pressure in a certain range, the more obvious the optimization effect is [10]. Arya et al. tried to improve machining quality using tube electrodes and investigated the correspondence between machining voltage and injection rate. It was found that at an appropriate injection rate, the tube electrode can refine the gas film while replenishing the electrolyte and taking away the machining products, achieving high quality machining of small holes [11]. Arya et al. analyzed the difference in material removal mechanism between tube electrode and cylindrical electrode. The experimental results showed that the machining efficiency was increased by 33.66% using the tube electrode compared

to the cylindrical electrode, and the entrance and exit dimensions of small holes were reduced from 1097 $\mu\text{m}$  and 698 $\mu\text{m}$  to 912 $\mu\text{m}$  and 616 $\mu\text{m}$ , respectively [12].

By applying ultrasonic vibration to the tool electrode, the resulting cavitation improves the flow field in the gap and enhances machining quality. Elhami et al. found that a moderate amount of ultrasonic vibration promotes the rate of gas film generation and reduces the thickness of the gas film [13–15]. Singh et al. analyzed the state of discharge energy transfer during ultrasonic-assisted electrochemical discharge machining and concluded that the addition of ultrasonic vibration increased the machining depth by a factor of two and reduced the discharge energy per unit time by 50% [16]. Rathore et al. studied the effect of ultrasonic vibration on electrochemical discharge machining. It was found that proper ultrasonic vibration can refine the gas film, promote the renewal of electrolyte in the machining gap, form a stable discharge, and ultimately improve the machining accuracy [17]. Rathore et al. analyzed the effect of ultrasonic vibration on material removal rate and electrode loss during electrochemical discharge machining, and established a mathematical model of material removal rate and electrode loss by means of dimensional analysis [18].

In this paper, ECDM is combined ultrasonic vibration with electrolyte injection to promote electrolyte circulation and improve machining quality, and the effects of parameters such as machining voltage, electrolyte injection rate, pulse frequency, and duty cycle on the machining effect are investigated to obtain the optimized machining parameters, and the array of small holes with high quality and large depth-diameter ratio are machined.

## 2 Machining principle

The principle of ultrasonic vibration electrochemical discharge machining is shown in Fig. 1. During the electrochemical machining of small holes, the hollow part of the tube electrode is used to inject electrolyte to the machining

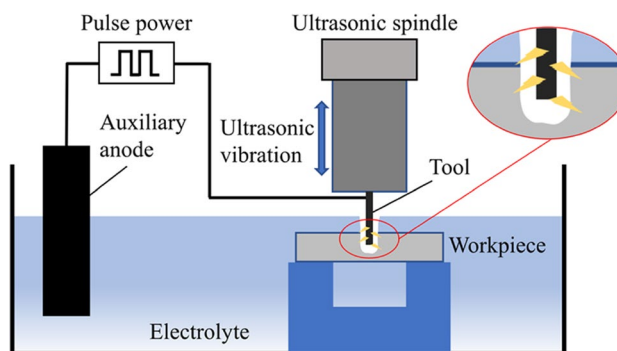


Fig. 1 Machining schematic

gap, as shown in Fig. 2. The electrolyte injection makes the pressure of the machining gap increase, and the electrolyte flows outward to disperse the gas bubbles accumulated at the entrance and side walls of the small hole, and binds the gas film to the electrode surface to form a uniform bubble film, so that the discharge process is smooth and continuous. After the machining starts, the tool electrode applies ultrasonic vibration in the vertical direction, which causes the electrode to make reciprocating motion in the vertical direction, prompting the electrolyte in the machining gap to produce periodic inhalation and exhalation, which is conducive to stable discharge.

### 3 Modeling simulation

#### 3.1 Simulation of the temperature field

The equilibrium discharge module in COMSOL is used to simulate the spark discharge process in electrochemical discharge machining and to analyze the state of heat distribution within the machining gap generated by the discharge of tube electrodes with different wall thicknesses. Before the simulation, the following assumptions were made to simplify the model:

- (1) The workpiece material is isotropic and homogeneous;
- (2) The technological conditions are constant in the process of machining;
- (3) The potential distribution in the electrolyte region satisfies Laplace’s equation.

The simulation model is shown in Fig. 3, in which the immersion depth is 0.3mm, the hole depth is 0.2mm, the side wall machining gap is 0.1 mm, the bottom machining gap is 0.05mm, the outer diameter of the tube electrode

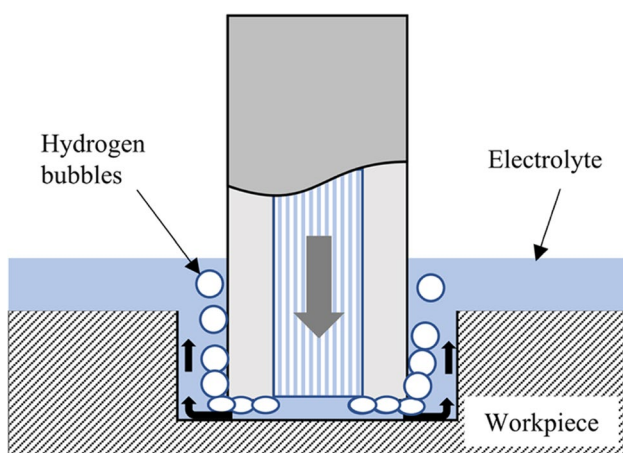


Fig. 2 Electrolyte injection schematic

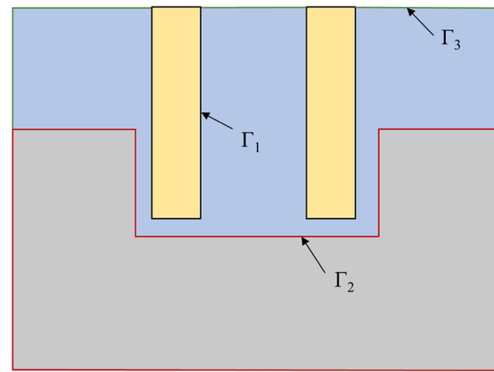


Fig. 3 Temperature field simulation model of single-hole tube electrode

is 1 mm, the inner diameters are 0.6 mm and 0.5mm, the electrode material is copper, the workpiece material is quartz glass, the electrolyte is KOH solution, the initial machining voltage in the machining area is 0V, and the initial temperature is 293K. The boundary  $\Gamma_1$  is the tool electrode boundary, the boundary  $\Gamma_2$  is the workpiece boundary, and the boundary  $\Gamma_3$  is the electrolyte boundary. The specific boundary conditions are shown in Eq. (1).

$$\begin{aligned} \Gamma_1 : \varphi|_{\Gamma_1} &= 0 \\ \Gamma_2 : \varphi|_{\Gamma_2} &= U = 60V \\ \Gamma_3 : \frac{\partial \varphi}{\partial n}|_{\Gamma_3} &= 0 \end{aligned} \tag{1}$$

The melting temperature of glass is 600–800°C. In this paper, it is assumed that the workpiece material will be removed when the temperature exceeds 800°C. The calculated temperature gradient diagram is shown in Fig. 4, and the yellow area is the area where the temperature reaches 800°C. The results show that when machining with a tube electrode, the discharge energy generated by the inner wall of the tube electrode cannot be transferred to the center of the electrode, and an island phenomenon is generated. When the inner diameter of the tube electrode is 0.6mm, the island diameter is about 330µm; when the inner diameter of the tube electrode is 0.5mm, the island diameter decreases to 210µm, but it can never be avoided. If the electrolyte injection is added to this, the island area may increase further, so the single-hole tube electrode is not suitable for small hole machining.

Comparing the electrode shapes, it can be seen that the porous tube electrode has a surface at the center of its end that can generate a gas film to form a spark discharge, so

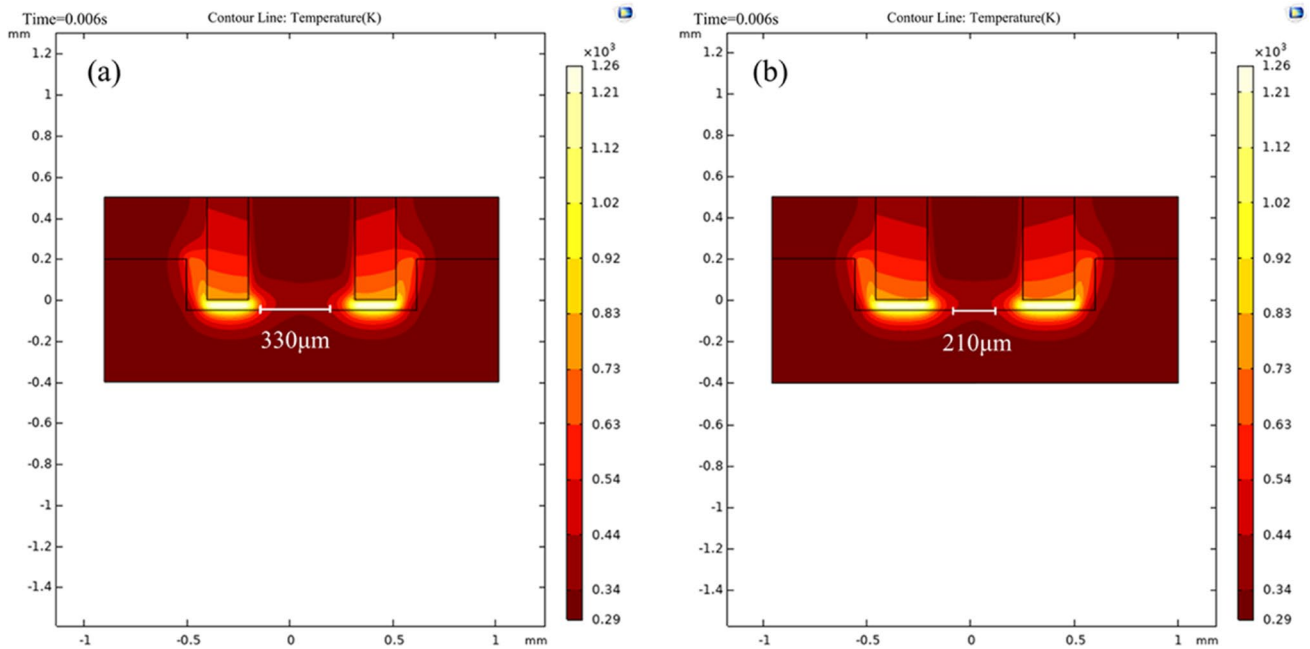


**Fig. 4** Simulation results of temperature field of single-hole tube electrode: **a** tube electrode with 0.6mm inner diameter; **b** tube electrode with 0.5mm inner diameter

theoretically, there will be no islands in the resulting small hole. Without changing other parameters, a porous tube electrode with 1mm outer diameter was used for simulation. The results are shown in Fig. 5, and it can be found that machining with a porous tube electrode can effectively

remove the material at the center of the hole and avoid the island phenomenon.

### 3.2 Simulation of the flow field

As shown in Fig. 6, a flow field simulation model was established to study the effect of coupling effect of ultrasonic vibration and electrolyte injection on the gas film. The inlet area is  $0.12\text{mm}^2$ , the distance between the side wall surface and the bottom surface of the tube electrode and the

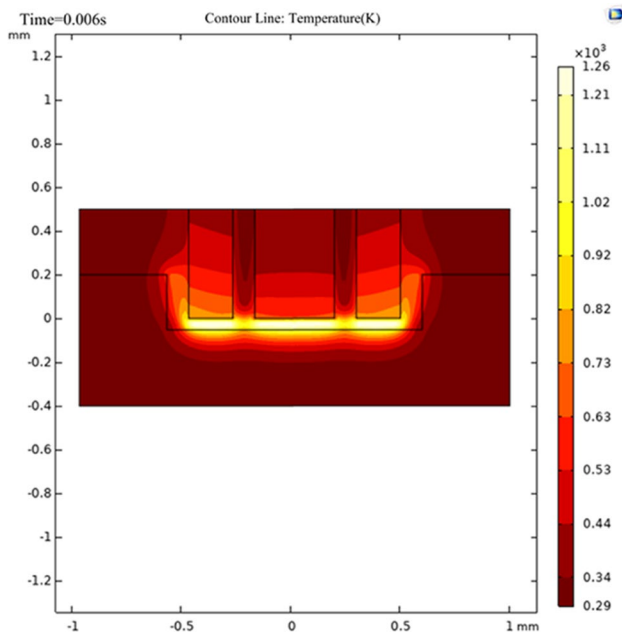


**Fig. 5** Temperature field simulation results of porous tube electrode

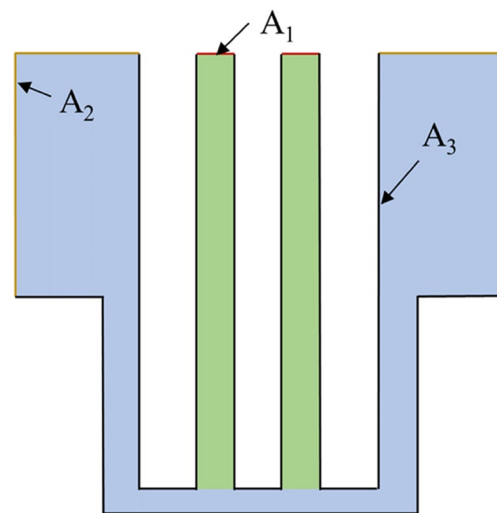


**Fig. 6** Simulation model of flow field of porous tube electrode

workpiece surface are 0.15mm and 0.1mm respectively, the electrolyte is KOH solution with 20% mass fraction, the ultrasonic amplitude is set to 7.5μm, and the frequency is 25kHz. Boundary A<sub>1</sub> is the velocity inlet, which simulates the inlet of the electrolyte injection of the porous tube electrode during the machining process, boundary A<sub>2</sub> is the pressure outlet, and boundary A<sub>3</sub> is the wall. The boundary A<sub>3</sub> is set to wall, and the specific boundary conditions are shown in Eq. (2).

$$A_1 : Q|_{A_1} = 0 \sim 120 \mu\text{l}/\text{min}$$

$$A_2 : \text{Pressure outlet} \tag{2}$$

$$A_3 : \text{Wall}$$

The simulation results are shown in Figs. 7 and 8. In the figure, the red part is the gas film layer required for effective discharge, and the other colors are the gas–liquid mixture. When ultrasonic vibration and electrolyte injection are not added (Fig. 7), the gas film is thicker and will contact with the hole side wall, which hinders the electrolyte circulation in the machining gap. When the electrolyte injection rate is 60μl/min (Fig. 8a), the flowing electrolyte starts to act on the flow field in the machining gap and binds the gas film on the surface of the tool electrode, and the thickness of the gas film decreases significantly and gradually separates from the side wall of the hole. After adding ultrasonic vibration (Fig. 8b), the electrolyte injection and ultrasonic vibration act together on the flow field in the machining gap, and the gas film is further refined and the thickness of the

gas film decreases. When the injection rate reaches 120μl/min (Fig. 8c), the effect of the electrolyte injection on the flow field in the machining gap is further increased, and the thickness of the gas film is significantly reduced. At this time, ultrasonic vibration is added (Fig. 8d), and the thickness of the gas film is almost unchanged under the extrusion of electrolyte.

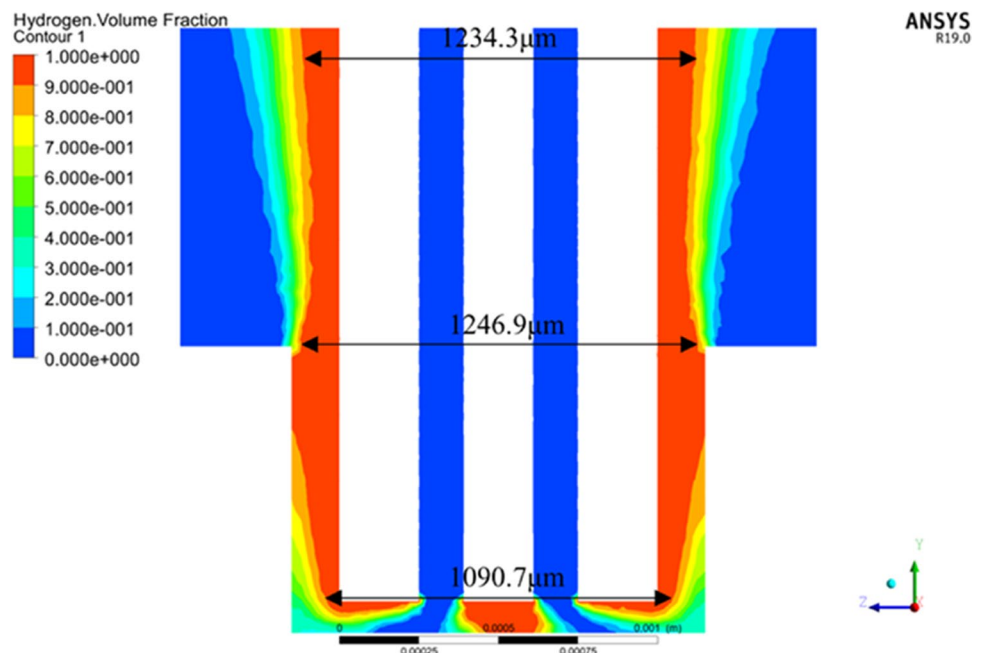
The simulation results show that when the electrolyte injection rate is less than 120μl/min, the electrolyte injection and ultrasonic vibration jointly refine the gas film on the electrode surface and optimize the machining quality. However, when the electrolyte injection rate exceeds 120μl/min, the interference of the electrolyte injection on the flow field inside the machining gap is obvious enough to greatly weaken the disturbance effect of ultrasonic vibration on the flow field, and at this time, ultrasonic vibration may not have any effect on the machining quality.

## 4 Experimental results and discussion

### 4.1 Experimental setup

The experimental platform is shown in Fig. 9. the X-, Y-, and Z-axis motions are mainly operated by the control software developed based on LabWindows/CVI, with the displacement speed of 0.1~10mm/s and the maximum travel of ±50mm. the ultrasonic spindle generates the axial motion with the frequency of 25 to 30kHz by the ultrasonic generator. The power supply is RS-12H30 pulse power supply, and its main output parameters are shown in Table 1. A CP8030H model Hall current sensor is used to record the current data

**Fig. 7** Simulation results of gas film thickness on the surface of the tube electrode without electrolyte injection and ultrasonic vibration



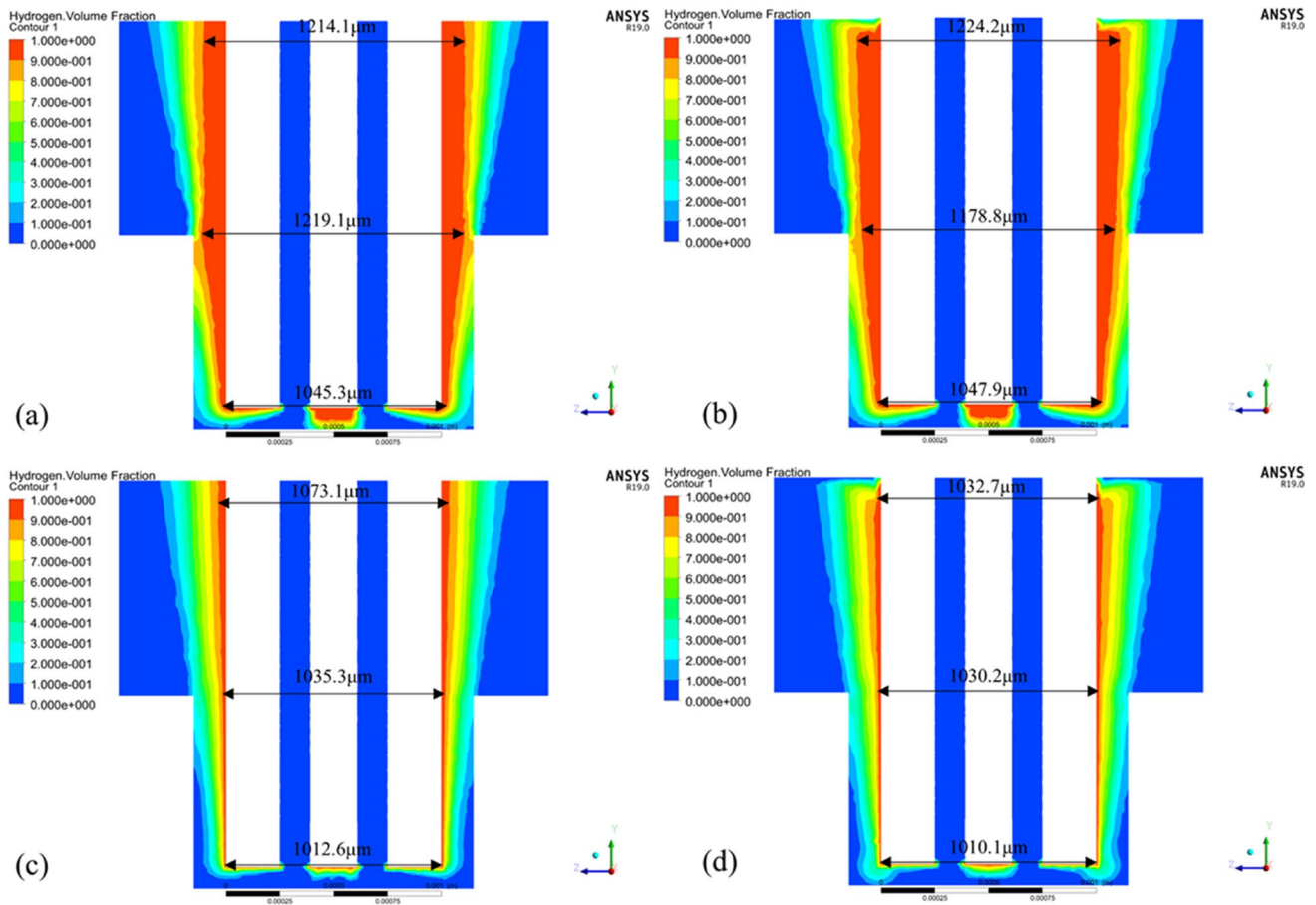


**Fig. 8** Simulation results of gas film thickness on the surface of tube electrode under the coupling effect of electrolyte injection and ultrasonic vibration: **a** small injection rate without ultrasonic; **b** small

injection rate with ultrasonic; **c** large injection rate without ultrasonic; **d** large injection rate with ultrasonic

under high frequency conditions, and the acquired data are converted into visual images by a TBS1104 oscilloscope. Nikon SMZ1270 optical microscope was used to observe

the machined small holes, and the 3D measurement and splicing measurement module of VK-X1000 laser confocal microscope was used to complete the 3D morphology

**Fig. 9** Experimental setup diagram

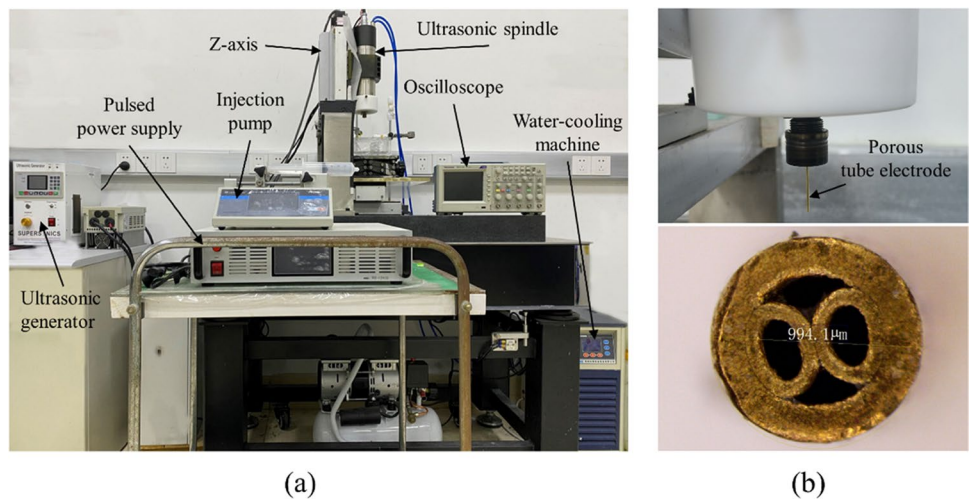


**Table 1** RS-12H30 pulse power output parameters

Parameter name	Parameter values
Pulse output form	Positive pulses
Peak output voltage	0~120V <sub>pp</sub> ±0.5%
Output peak current	<30A±0.5%
Frequency of output	10Hz~200kHz
Pulse width	10~90%

measurement of the small holes. The Rave TYDO1-01 micro flow syringe pump was used as the liquid supply pump, and the BD Plastic 60ml syringe was used to reserve alkaline electrolyte.

### 4.2 Study on the machining quality of single-hole tube electrode

The tube electrodes of 1mm outer diameter and 0.6mm and 0.5mm inner diameter are selected for machining experiments. The experimental voltage is 60V, the frequency is 10kHz, the duty cycle is 70%, the feed rate of the electrode is 10µm/s, and the machining depth is 500µm.

The experimental results are shown in Fig. 10. There is an obvious island phenomenon at the center of the small hole. The island diameter was 502.6µm when the inner diameter of the tube electrode was 0.6 mm, and it decreased to 402.5µm when the inner diameter of the tube electrode was 0.5 mm. Even if the inner diameter of the tube electrode was

further reduced for the experiment, the island phenomenon was always present.

### 4.3 The effect of electrolyte injection rate and electrical parameters on machining quality

In this experiment, an L25(5<sup>4</sup>) orthogonal experiment was designed to investigate the effects of the electrolyte injection rate and electrical parameters on the machining quality during the electrochemical discharge machining of the tube electrode, and to analyze the importance of the variation of the electrolyte injection rate, voltage, duty cycle, and pulse frequency on the entrance size and machining depth. The workpiece used in the experiment was a 36.5 mm × 36.5 mm × 5 mm super white glass with a feed rate of 20 µm/s. The electrolyte was a 20% mass fraction KOH solution. The experimental parameters are shown in Table 2, and the experimental setup and experimental results are shown in Table 3.

As shown in Tables 4 and 5, the order of the weight of the four factors on the machining quality is A>C>B>D, that is, machining voltage> pulse frequency> duty cycle> electrolyte injection rate, whether it is machining depth or depth-diameter ratio. The parameter group with the largest machining depth is A<sub>1</sub>C<sub>4</sub>B<sub>3</sub>D<sub>3</sub>, and the parameter group with the largest depth-diameter ratio is A<sub>1</sub>C<sub>5</sub>B<sub>4</sub>D<sub>2</sub>. Further analysis of the results of comparison tests 12, 16, and 25 shows that the same electrolyte injection rate for different electrical parameters, the effect of the effect may be changed from refining the gas film to too much pressure makes the

**Fig. 10** Single-hole tube electrode machining results: **a** inner diameter of 0.6mm; **b** inner diameter of 0.5mm

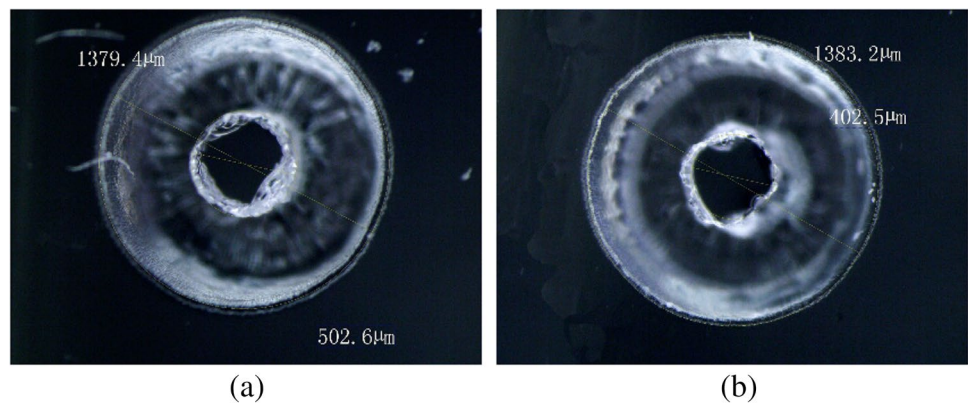


**Table 2** Matrix of factors and levels

Factors	Code	Levels				
		1	2	3	4	5
Machining voltage (V)	A	80	75	70	65	60
Impulse frequency (kHz)	B	50	75	100	125	150
Duty cycle (%)	C	45	50	55	60	65
Injection rate (µl/min)	D	0	30	60	90	120

**Table 3** L25(5<sup>4</sup>) Table of orthogonal arrays and results

No.	A	B	C	D	Diameter (μm)	Depth (μm)	Depth-diameter ratio
1	1	1	1	1	1802.95	1209.23	0.67
2	1	2	3	4	1730.05	1545.96	0.91
3	1	3	5	2	2027.5	2106.7	1.06
4	1	4	2	5	1798.35	1665.02	0.92
5	1	5	4	3	1688.45	2305.63	1.05
6	2	1	5	4	1885.55	1435.1	1.06
7	2	2	2	2	1727.1	1499.12	0.87
8	2	3	4	5	1868.45	1939.07	1.03
9	2	4	1	3	1763.95	1486.62	0.82
10	2	5	3	1	2148.2	1624.56	0.74
11	3	1	4	2	1741.53	1377.73	0.78
12	3	2	1	5	1374.9	385.46	0.25
13	3	3	3	3	1868.85	1603.94	0.86
14	3	4	5	1	2046.35	1870.28	0.92
15	3	5	2	4	1768.05	1679.9	0.96
16	4	1	3	5	1323.55	522.57	0.40
17	4	2	5	3	1651.15	1516.54	0.91
18	4	3	2	1	1575.15	1126.65	0.70
19	4	4	4	4	1521	1471.57	0.97
20	4	5	1	2	1558.45	1317.07	0.82
21	5	1	2	3	1331.5	538.05	0.23
22	5	2	4	1	1544.35	999.92	0.63
23	5	3	1	4	1204.1	168.34	0.15
24	5	4	3	2	1564.5	1044.96	0.66
25	5	5	5	5	1523.45	1058.75	0.69

**Table 4** Analysis of the machining depth

Sum at each level	Factors			
	A	B	C	D
$K_1$	8832.54	5082.68	4566.72	6830.63
$K_2$	7984.48	5947.00	6508.74	7345.58
$K_3$	6917.30	6944.70	6341.99	7450.78
$K_4$	5954.40	7538.45	8093.91	6300.86
$K_5$	3810.02	7985.91	7987.37	5570.89
$R$	5022.53	2903.23	3527.19	1774.69

**Table 5** Analysis of the depth–diameter ratio

Sum at each level	Factors			
	A	B	C	D
$K_1$	4.60	3.13	2.71	3.66
$K_2$	4.53	3.57	3.67	4.18
$K_3$	3.76	3.79	3.56	3.86
$K_4$	3.79	4.28	4.45	4.05
$K_5$	2.35	4.26	4.64	3.29
$R$	2.26	1.15	1.92	0.89

gas film is scattered to produce a stable discharge. Therefore, the optimized parameter group  $A_1C_4B_4D_4$  (80V, 125kHz, 65%, 90μl/min) was selected under the premise of ensuring the maximum depth and depth–diameter ratio.

#### 4.3.1 The effect of electrolyte injection rate and machining voltage on machining quality

The pulse frequency of 125kHz, duty cycle of 60%, voltage of 71–80V, electrolyte injection rate of 0–150μl/min, and machining feed rate of 10μm/s were chosen to study the effect of electrolyte injection rate and machining voltage on the machining quality of small holes, and the experimental results are shown in Fig. 11. With the increasing rate of electrolyte injection, the entrance size of small hole will gradually decrease, while the machining depth of small hole is showing a trend of first increasing and then decreasing. Due to the different bubble generation rates and discharge conditions at different voltages, the electrolyte injection rate corresponding to the maximum machining depth is also different.



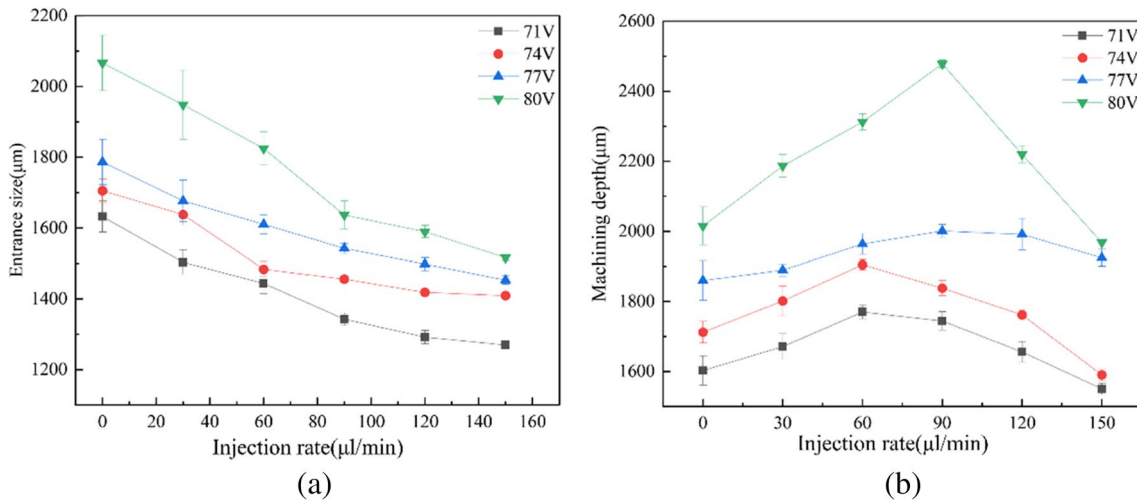
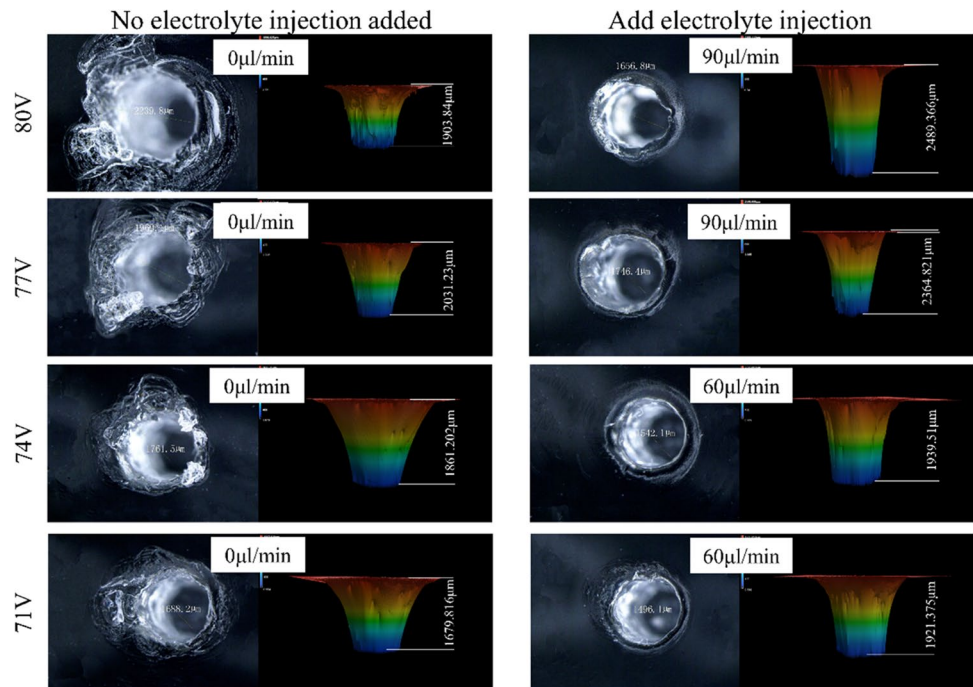


**Fig. 11** Experimental results of the effect of electrolyte injection and machining voltage on machining quality: **a** effect on the entrance size; **b** effect on the machining depth

The three-dimensional morphology of the small holes machined at different voltages without and with the optimized electrolyte injection rate is shown in Fig. 12. It can be observed that when the machining voltage is 80V and the electrolyte injection rate is 0, extreme discharge occurs during the machining process, and the high temperature generated by the discharge heats the material at the entrance to a molten state and spreads in all directions, resulting in broken-like defects. As the voltage decreases, the extreme discharge phenomenon then decreases and the entrance size

of the small holes and the surrounding breakage defects are significantly reduced. In addition, the electrolyte injection rate can reduce the sidewall taper of the small hole while improving the machining accuracy and depth, because the electrolyte injection improves the gas film thickness and electrolyte circulation by affecting the flow field in the machining gap, and reduces the effect of sidewall discharge on machining within a certain depth range. Based on the machining depth and depth–diameter ratio, the optimized machining voltage parameter is 80V. Under the effect of the

**Fig. 12** Machining results at different electrolyte injection rates and voltages



injection rate of 90 $\mu$ l/min, the average depth of small holes is 2478.19 $\mu$ m and the depth–diameter ratio is 1.49.

### 4.3.2 The effect of electrolyte injection rate and pulse frequency on machining quality

A voltage of 80V and a pulse frequency of 5–150kHz were chosen, and other machining parameters were kept constant to study the effects of the electrolyte injection rate and pulse frequency on the machining quality of small holes. The current waveforms at different pulse frequencies are shown in Fig. 13. The higher current peak indicates the stronger electrolysis and the thicker gas film generated. The overly thick gas film will prevent the discharge energy from transferring to the workpiece surface, resulting in a reduced material removal rate. From the figure, the peak current gradually decreases as the pulse frequency increases and the discharge process becomes stable.

The pulse frequency of 100–137.5kHz is selected for further experiments, and the experimental results are shown in Fig. 14. As the pulse frequency increases, the entrance size of the small hole increases, while the machining depth tends to increase and then decrease with the increase of pulse frequency.

The three-dimensional morphology of the small holes machined without and at the optimized electrolyte injection rate at different pulse frequencies is shown in Fig. 15.

As the frequency increases, the possibility of extreme discharges increases and the distribution of discharge points becomes more uneven, so the entrance defects gradually change from a circular heat affected zone to a less rounded and more extensive broken heat affected zone. Although the machining depth increases, the sidewall taper of the small hole gradually increases with frequency without the addition of the electrolyte injection because of the increased chance of sidewall discharge. After the electrolyte injection is introduced into the machining gap, the flow field perturbation provided by it stabilizes the thickness and uniformity of the gas film and improves the roundness of the small hole. At the same time, the electrolyte injection replenishes the electrolyte consumed in the machining gap while taking away the machining products and sidewall discharge energy, providing conditions for continuous generation of spark discharge, which greatly improves machining stability and machining accuracy. When the electrolyte injection rate continues to increase, the excessive gap pressure will destroy the gas film stability, and although the entrance size will still be reduced, the machining depth will not be guaranteed. According to the machining depth and depth–diameter ratio, 125 kHz is the optimized machining pulse frequency, and the average depth of 2478.19 $\mu$ m and the depth–diameter ratio of 1.49 are obtained under the action of 90 $\mu$ l/min electrolyte injection rate.

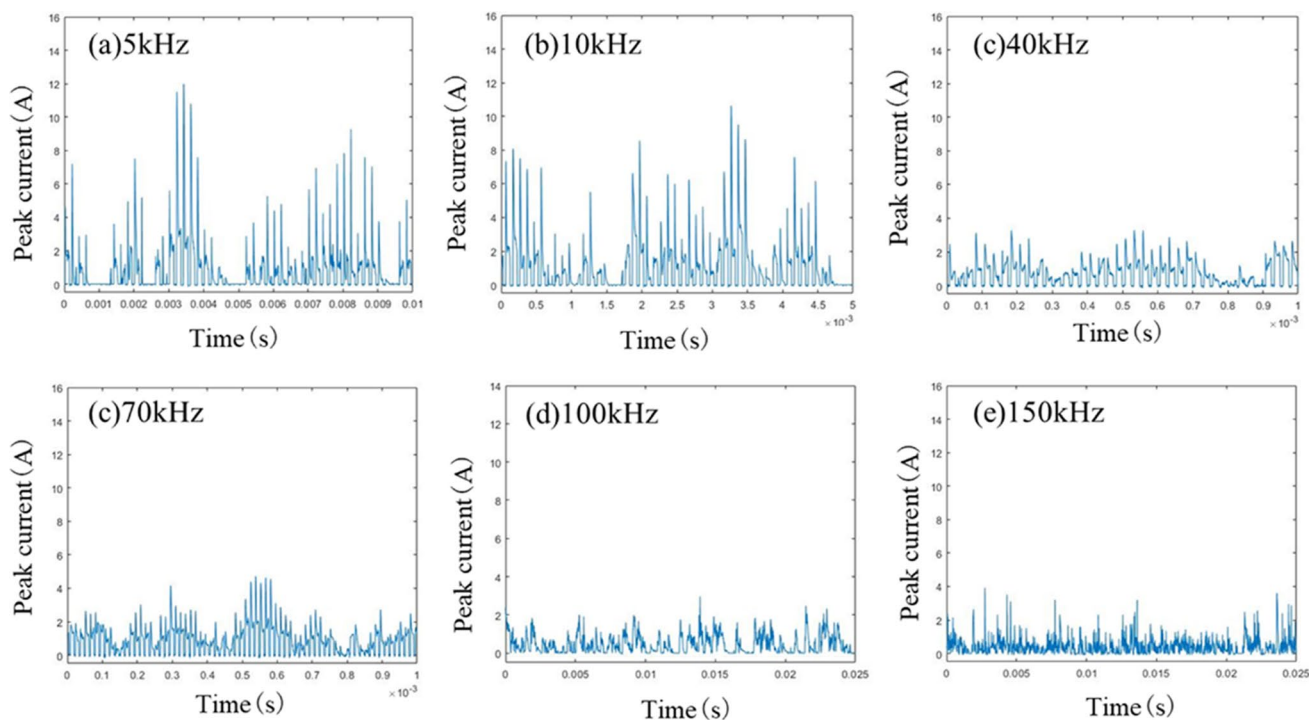
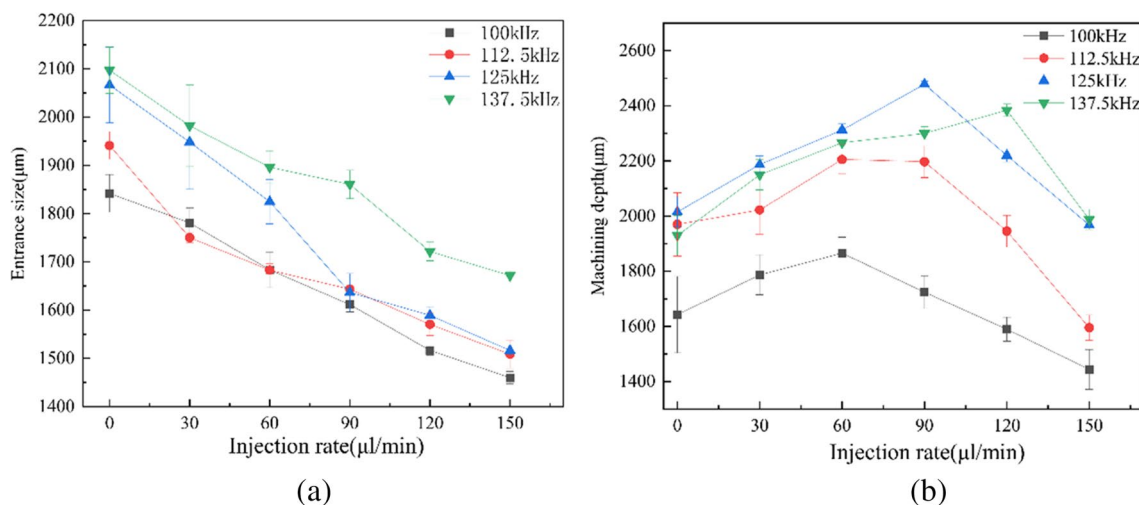
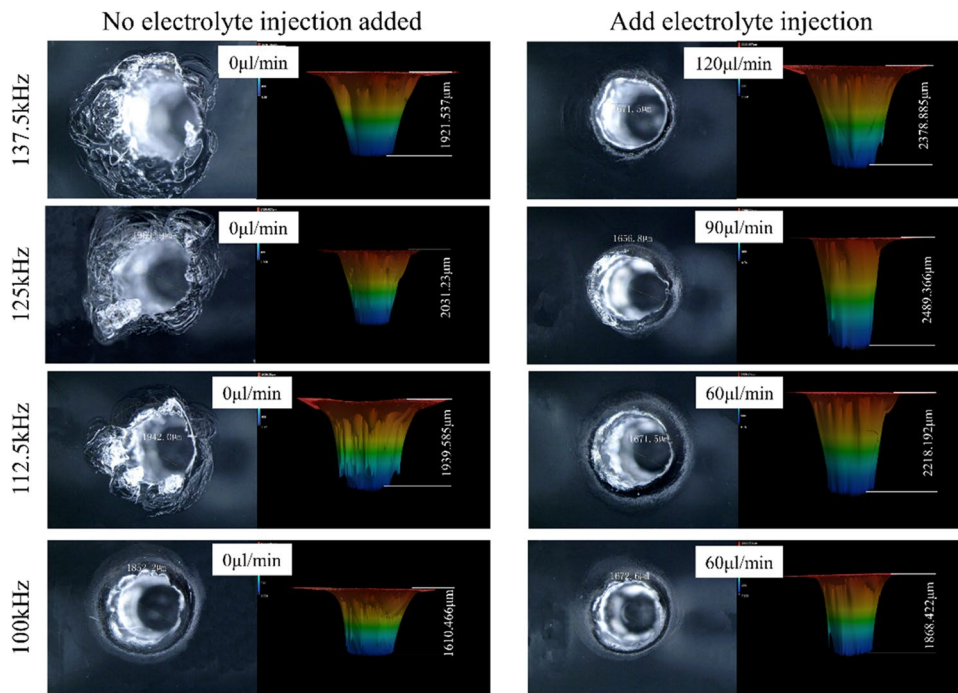


Fig. 13 Current waveforms at different pulse frequencies



**Fig. 14** Experimental results of the effect of electrolyte injection rate and pulse frequency on machining quality: **a** effect on entrance size; **b** effect on machining depth

**Fig. 15** Machining effect at different electrolyte injection rate and pulse frequency



### 4.3.3 The effect of electrolyte injection rate and duty cycle on machining quality

The machining voltage was chosen to be 80V, the pulse frequency was 125kHz, the duty cycle was 55–70%, and other machining parameters were kept constant to study the effect of the electrolyte injection rate and duty cycle on the quality of small hole machining, and the experimental results are shown in Fig. 16. Duty cycle by controlling the pulse width ratio to change the single pulse cycle to

generate spark discharge time. The larger the duty cycle, the higher the probability of generating multiple spark discharges within a single pulse cycle, and the increase in the total number of discharges results in a corresponding increase in the material removal rate. However, when the electrolyte injection rate exceeds a certain range, the material removal rate decreases because the stable gas film required for the discharge is destroyed by the large pressure, and the machining depth tends to decrease.

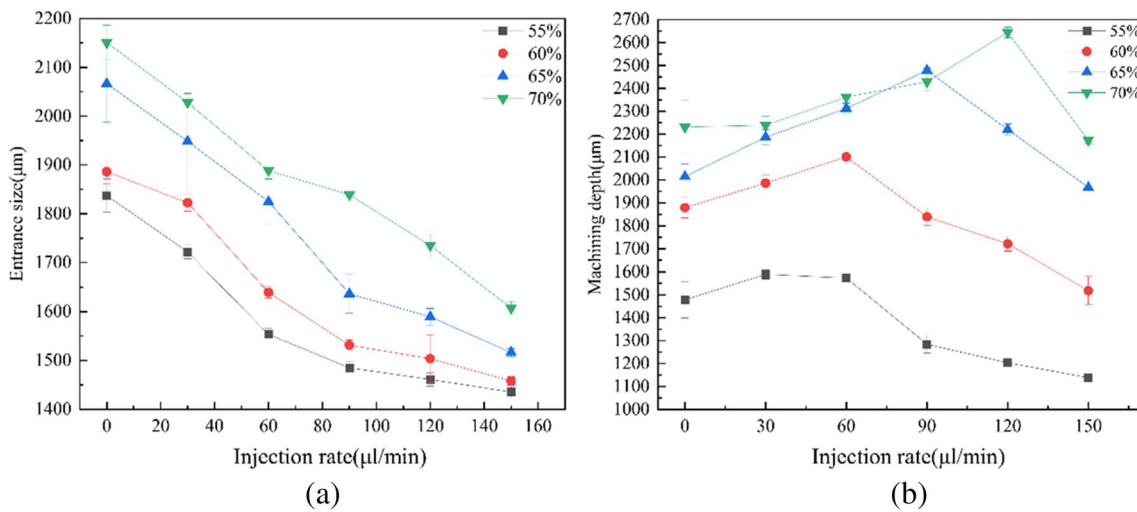


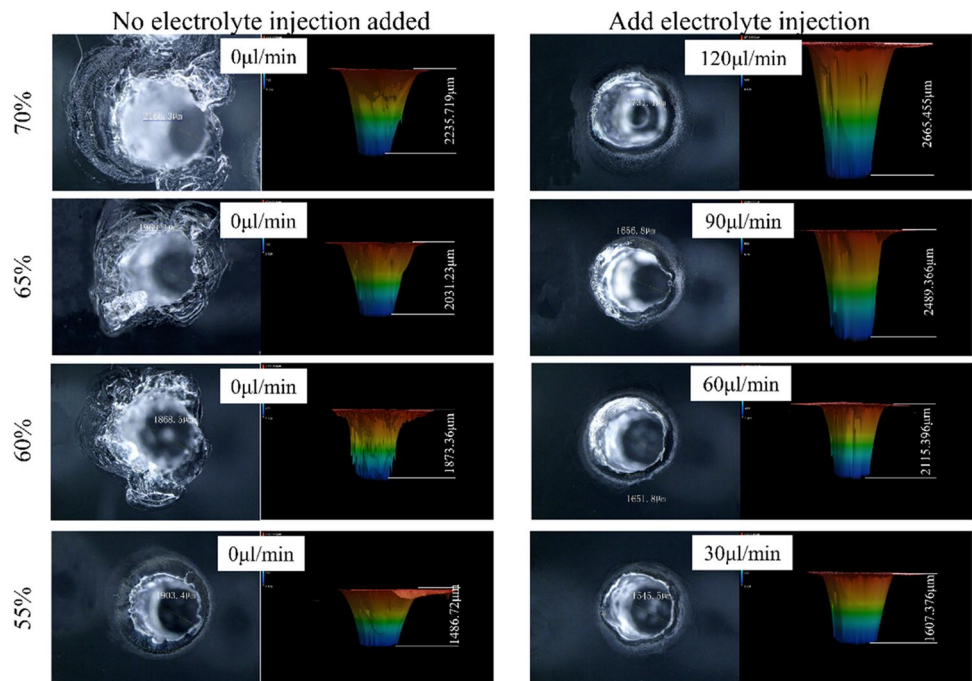
**Fig. 16** Experimental results of the effect of electrolyte injection rate and duty cycle on machining quality: **a** effect on entrance size; **b** effect on machining depth

The three-dimensional morphology of the small holes machined without and with the optimized electrolyte injection rate at different pulse frequencies is shown in Fig. 17. It can be seen that the machining quality is significantly improved after adding the electrolyte injection. This is due to the fact that the electrolyte injection takes away the discharge energy originally transferred to the side wall of the small hole for secondary machining, and at the same time binds the gas film on the electrode surface, making the discharge process stable. According to the machining depth

and depth–diameter ratio, 70% is the optimized machining duty cycle, and the average depth of 2644.13μm and the depth–diameter ratio of 1.52 are obtained under the action of 120μl/min of the electrolyte injection rate.

The optimized combination of machining parameters was obtained as follows: machining voltage of 80V, pulse frequency of 125kHz, duty cycle of 70%, and electrolyte injection rate of 120μl/min. Compared with no electrolyte injection, the average entrance size of small holes

**Fig. 17** Machining effect at different electrolyte injection rate and duty cycle



decreased from 2150.8 to 1734.9 $\mu\text{m}$ , the average machining depth increased from 2230.78 $\mu\text{m}$  to 2644.13 $\mu\text{m}$ , and the depth-to-diameter ratio increased from 1.04 to 1.52, and the depth–diameter ratio increased from 1.04 to 1.52.

#### 4.4 The effect of ultrasonic vibration on machining quality

Through the previous experimental study, the optimized combination of parameters for machining array of small holes and small holes with large depth–diameter ratio was obtained respectively. Based on the optimized machining parameter set, ultrasonic vibration was introduced to study its effect law on machining quality. The experimental parameters are set as shown in Table 6.

The experimental results are shown in Fig. 18. When the ultrasonic amplitude gradually increases from 0 to 7 $\mu\text{m}$ , the entrance size of the small hole shows a gradual decrease and the machining depth shows a gradual increase. When the electrolyte injection rate is 30 $\mu\text{l}/\text{min}$ , the entrance size decreases from 1488.3 to 1376.6 $\mu\text{m}$ , and the machining depth increases from 501.9 to 589.6 $\mu\text{m}$ .

**Table 6** Machining parameters table

Group	1	2	3	4
Ultrasonic amplitude ( $\mu\text{m}$ )	0–7	0–7	0–7	0–7
Injection rate ( $\mu\text{l}/\text{min}$ )	30	60	90	120
Machining voltage (V)	80	80	80	80
Duty cycle (%)	70	70	70	70
Pulse frequency (kHz)	125	125	125	125
Feed rate ( $\mu\text{m}/\text{s}$ )	20	20	20	20

This is due to the ultrasonic vibration on the flow field in the gap, the perturbing effect of ultrasonic vibration periodically draws in and discharges electrolyte, so the gas film is bound, and its thickness decreases accordingly. In addition, the periodic flow of electrolyte can flush out the gas bubbles gathered at the entrance of the small hole, which to some extent alleviates the spark discharge discontinuity and improves the machining stability.

The current waveforms during discharge of the group 1 are shown in Fig. 19. As the ultrasonic amplitude increases from 0 to 7 $\mu\text{m}$ , on the one hand, the first higher current peak in the cycle decreases, and the peak floating range of adjacent cycles also decreases significantly, indicating that the time required from electrolysis to gas film generation under ultrasonic perturbation becomes shorter, and the thickness of gas film generated in adjacent cycles becomes more uniform, so that the roundness and accuracy of the resulting small holes are higher. On the other hand, the peak and average currents of spark discharge during the cycle are gradually reduced, which indicates that the energy of discharge generated during the cycle is reduced and the stability of discharge is significantly improved, so that the stability of the machining process is higher and the dimensional accuracy of the resulting small holes is further improved.

However, when the electrolyte injection rate exceeds 90 $\mu\text{l}/\text{min}$ , the effect of ultrasonic vibration is significantly weakened, especially when the electrolyte injection rate reaches 120 $\mu\text{l}/\text{min}$ , ultrasonic vibration has almost no effect. This is because the pressure and injection rate in the machining gap are too large, which greatly weaken the disturbing effect of ultrasonic vibration and make the effect of ultrasonic vibration on the gas film cannot be

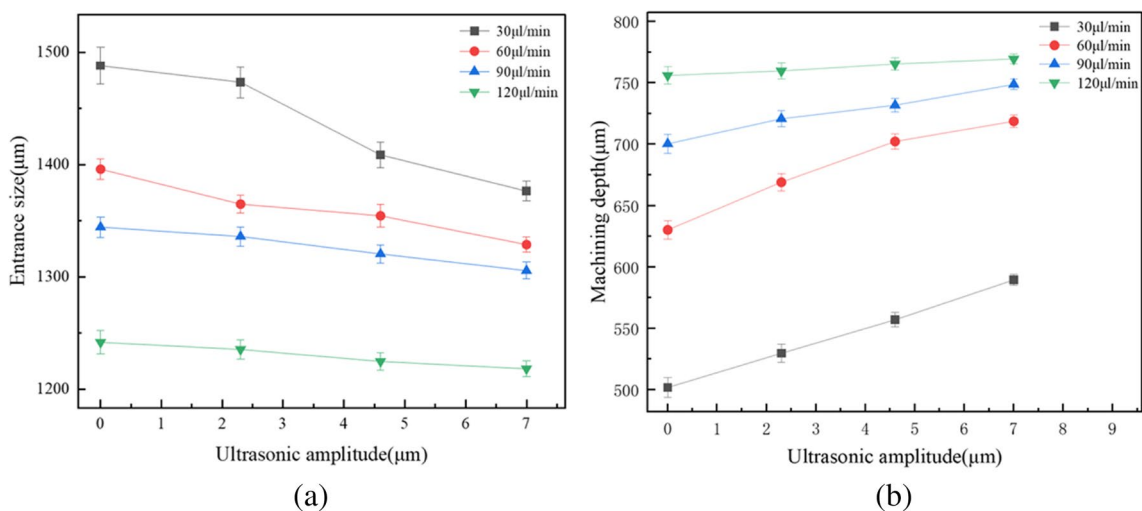


**Fig. 18** Experimental results of the effect of electrolyte injection rate and ultrasonic amplitude on machining quality: **a** effect on entrance size; **b** effect on machining depth

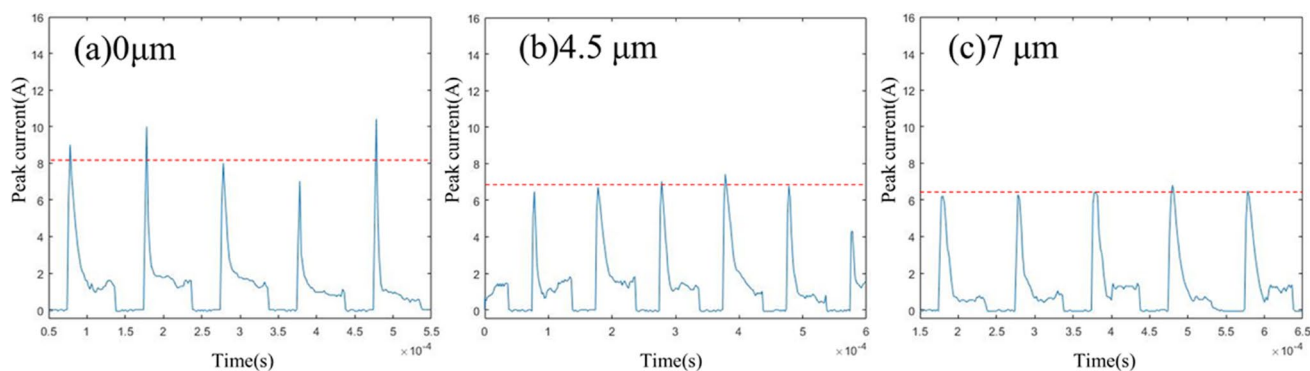


Fig. 19 Current waveform under ultrasonic vibration

reflected, so ultrasonic vibration has almost no effect on the machining effect.

#### 4.5 Typical workpiece machining

The experimental analysis shows that a voltage of 80V, a duty cycle of 70%, a frequency of 125kHz, an electrolyte injection rate of 30 $\mu$ l/min, a feed rate of 20 $\mu$ m/s, and an ultrasonic amplitude of 7 $\mu$ m are the optimized combination of parameters for machining the array of small holes. A 5 $\times$ 5 array hole structure with an average entrance size of 1380 $\pm$ 5 $\mu$ m and an average machining depth of 600 $\mu$ m $\pm$ 10 $\mu$ m was obtained, and the machining time of a single small hole was 30s, as shown in Fig. 20.

A voltage of 80 V, a duty cycle of 70%, a frequency of 125 kHz, an electrolyte injection rate of 120 $\mu$ l/min, a feed rate of 20 $\mu$ m/s, and an ultrasonic amplitude of 7 $\mu$ m are the optimized combination of parameters for machining small holes with a large depth-diameter ratio. The average entrance size of 1670 $\pm$ 20 $\mu$ m, the average machining depth of 3030 $\pm$ 20 $\mu$ m and the depth-diameter ratio of 1.81 were

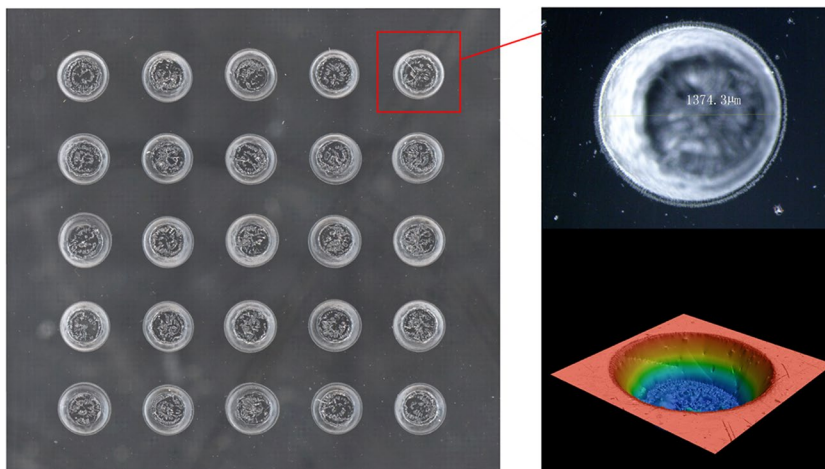
obtained, and the machining time of a single small hole was 300s, as shown in Fig. 21.

## 5 Conclusion

In order to solve the problem of electrolyte circulation during small-hole machining, this paper proposes the use of liquid injection inside the tube electrode and ultrasonic vibration for efficient and high-quality small-hole machining. Based on theory and experiment, the following conclusions can be obtained:

- (1) The simulation results show that the use of porous tube electrode machining can effectively remove the material at the center of the small hole and avoid the island phenomenon. In addition, the coupling effect of the electrolyte injection and ultrasonic vibration can refine the gas film on the electrode surface.
- (2) The orthogonal experiment determined the influence weight of four factors on the machining quality as:

Fig. 20 5 $\times$ 5 array of holes



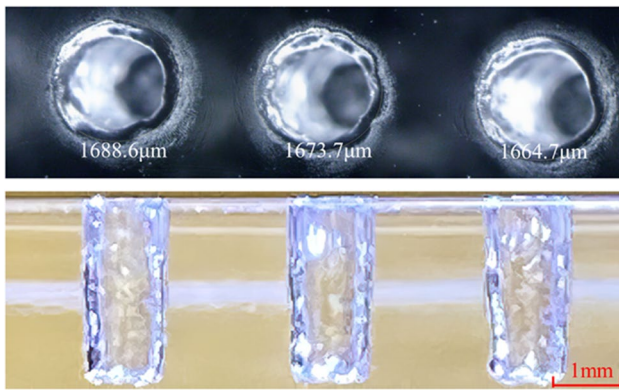


**Fig. 21** Small hole with large depth–diameter ratio

machining voltage > pulse frequency > duty cycle > electrolyte injection rate, and the best combination of machining parameters was: machining voltage of 80V, pulse frequency of 125kHz, duty cycle of 70%, and electrolyte injection rate of 120 $\mu$ l/min.

- (3) Machining of the glass small hole structure, compared with the traditional ECDM, the entrance size was reduced by 19.3%, the machining depth was increased by 18.5%, and the depth–diameter ratio was increased by 46.2%, which verified the effectiveness of liquid injection inside the tube electrode.
- (4) Ultrasonic vibration can improve machining quality under low-pressure and low-injection rate machining conditions, but has little effect under high-pressure and high-injection rate machining conditions.
- (5) A 5 $\times$ 5 array of small holes with an average entrance size of 1380 $\pm$ 5 $\mu$ m and an average depth of 600  $\mu$ m $\pm$ 10 $\mu$ m and a large depth–diameter ratio of small holes with an average entrance size of 1670 $\pm$ 20 $\mu$ m and small holes with an average machining depth of 3030 $\pm$ 20 $\mu$ m and a depth–diameter ratio of 1.81 were machined.

It has been proved that electrochemical discharge machining with ultrasonic vibrating tube electrodes can be an efficient method for machining glass small-hole structures with high quality. In future work, electrochemical discharge drilling and grinding combined with plated abrasive tube electrodes will be further investigated in order to obtain better machining quality.

**Code availability** Not applicable.

**Author contributions** Chenghu Jia performed the experiment, the data analyses, and wrote the manuscript; Yong Liu contributed to the conception of the study and edited the manuscript; others helped perform the analysis with constructive discussions.

**Funding** The authors acknowledge financial support from the National Key R&D Program of China (No. 2018YFB2001400), the National Natural Science Foundation of China (No. 52005298), and the Natural Science Foundation of Shandong Province (No. ZR2021ME048). This work is supported by Physical-Chemical Materials Analytical & Testing Center of Shandong University at Weihai.

**Data Availability** All data generated or analyzed during this study are included within the article.

## Declarations

**Ethics approval** This paper is in compliance with ethical standards.

**Consent to participate** All authors agreed with the consent to participate.

**Consent for publication** All authors have read and agreed to the publication of the paper.

**Competing interests** The authors declare no competing interests.

## References

1. Wang XL, Gao XD, Zhang ZH, Cheng LS, Ma HP, Yang WM (2021) Advances in modifications and high-temperature applications of silicon carbide ceramic matrix composites in aerospace: a focused review. *J Eur Ceram Soc* 41(9):4671–4688
2. Kang XM, Tang WD, Zhao WS, Qian J, Lauwers B (2021) Experimental and numerical investigations of material removal process in electrochemical discharge machining of glass in discharge regime. *Precis Eng* 72:706–716
3. Sharma P, Mishra DK, Dixit P (2020) Experimental investigations into alumina ceramic micromachining by electrochemical discharge machining process. *Procedia Manuf* 48:244–250
4. Singh M, Singh S, Kumar S (2020) Experimental investigation for generation of micro-holes on silicon wafer using electrochemical discharge machining process. *Silicon* 12(7):1683–1689
5. Kolhekar KR, Sundaram M (2018) Study of gas film characterization and its effect in electrochemical discharge machining. *Precis Eng* 53:203–211
6. Sabahi N, Razfar MR (2018) Investigating the effect of mixed alkaline electrolyte (NaOH + KOH) on the improvement of machining efficiency in 2D electrochemical discharge machining (ECDM). *Int J Adv Manuf Technol* 95(1-4):643–657
7. Elhami S, Razfar MR (2020) Application of nano electrolyte in the electrochemical discharge machining process. *Precis Eng* 64:34–44
8. Bian JX, Ma BJ, Liu XF, Qi LJ (2020) Experimental study of tool wear in electrochemical discharge machining. *Appl Sci* 10(15):5039
9. Sharma P, Dixit P (2022) Investigation of tool wear in alumina micromachining by multi-tip ECDM. *Mater Manuf Process* 37(3):342–348
10. Mehrabi F, Farahnakian M, Elhami S, Razfar MR (2018) Application of electrolyte injection to the electro-chemical discharge machining (ECDM) on the optical glass. *J Mater Process Technol* 255:665–672
11. Arya RK, Dvivedi A (2019) Investigations on quantification and replenishment of vaporized electrolyte during deep micro-holes drilling using pressurized flow-ECDM process. *J Mater Process Technol* 266:217–229

12. Arya RK, Dvivedi A (2019) Enhancement in machining efficiency and accuracy of ECDM process using hollow tool electrode. Springer Singapore, Singapore, pp 313–323
13. Elhami S, Razfar MR (2018) Effect of ultrasonic vibration on the single discharge of electrochemical discharge machining. *Mater Manuf Process* 33(4):444–451
14. Elhami S, Razfar MR (2017) Study of the current signal and material removal during ultrasonic-assisted electrochemical discharge machining. *Int J Adv Manuf Technol* 92(5-8):1591–1599
15. Elhami S, Razfar MR (2017) Analytical and experimental study on the integration of ultrasonically vibrated tool into the micro electro-chemical discharge drilling. *Precis Eng* 47:424–433
16. Singh T, Dvivedi A, Shanu A, Dixit P (2021) Experimental investigations of energy channelization behavior in ultrasonic assisted electrochemical discharge machining. *J Mater Process Technol* 293:117084
17. Rathore RS, Dvivedi A (2020) Sonication of tool electrode for utilizing high discharge energy during ECDM. *Mater Manuf Process* 35(4):415–429
18. Rathore RS, Dvivedi A (2020) Experimental investigations and its dimensional analysis-based modeling of the UAECDM process. *Int J Adv Manuf Technol* 111(11-12):3241–3257

**Publisher's note** Springer Nature remains neutral with regard to jurisdictional claims in published maps and institutional affiliations.

Springer Nature or its licensor (e.g. a society or other partner) holds exclusive rights to this article under a publishing agreement with the author(s) or other rightsholder(s); author self-archiving of the accepted manuscript version of this article is solely governed by the terms of such publishing agreement and applicable law.